Lab on a Chip

Accepted Manuscript

ROYAL SOCIETY OF CHEMISTRY

www.rsc.org/loc

Lab on a chip

RSCPublishing

ARTICLE

Artificial Blood Vessel Implanted Three-Dimensional Microsystem for Modeling Transvascular Migration of Tumor Cells

1Cite this: DOI: 10.1039/xoxxoooooox

Received ooth,
Accepted ooth

DOI: 10.1039/xoxxoooooox

www.rsc.org/

Xue-Ying Wang[a,&], *Ying Pei*[b,&], *Min Xie*[a], *Zi-He Jin*[a], *Ya-Shi Xiao*[a], *Yang Wang*[a], *Li-Na Zhang*[b], *Yan Li*[c] *and Wei-Hua Huang*[a*]

Reproducing tumor microenvironment consisting of blood vessels and tumor cells for modeling tumor invasion *in vitro* is particularly challenging. Here, we report an artificial blood vessel implanted 3D microfluidic system for reproducing transvascular migration of tumor cells. The transparent, porous and elastic artificial blood vessels are obtained by constructing polysaccharide cellulose-based microtubes using chitosan sacrificial template, and possess excellent cytocompatibility, permeability, and mechanical characteristics. The artificial blood vessels are then fully implanted into collagen matrix to reconstruct the 3D microsystem for modeling transvascular migration of tumor cells. Well-defined simulated vascular lumens were obtained by proliferation of the human umbilical vein endothelial cells (HUVECs) lining the artificial blood vessels, which enables us to reproduce structures and functions of blood vessel and replicate various hemodynamic parameters. Based on this model, the adhesion and transvascular migration of tumor cells across the artificial blood vessel have been well reproduced.

Introduction

Despite great advances in early diagnostics and therapy, cancer remains the leading cause of death mainly due to tumor invasion and metastasis[1,2]. Although studies on tumor invasion have provided much useful information, the invasion cascades are still far from being completely understood[2-4]. The entry of tumor cells into blood vessels is an important route of penetrating into the circulatory system and subsequently metastasizing to another organ through blood vessel walls[5,6]. However, studies of tumor invasion *in vivo* allow only limited control of physical, chemical, and biological factors and face challenges in observation with high spatial and temporal resolution[7,8]. Therefore, *In vitro* models to simulate 3D tumor microenvironment consisting of functional vasculature have emerged to be significant alternative approaches for elucidating process and mechanisms of transvascular migration of tumor cells[5,9,10].

Synthetic materials such as silicone tube were initially used to mimic blood vessels *in vitro*[11], but its poor permeability and compatibility restrict its further applications. Furthermore, there are a few successful examples showing that functional vasculature could be *in vitro* generated from preexisting vascular explants[12,13]. Recently, microfabrication techniques have been developed as powerful tools for the investigation of blood vessels[9]. Endothelial cells (ECs) were cultured on PDMS membranes enabling reconstitution of functional interfaces of blood vessel, which would accelerate investigation the diagnosis and treatment of vascular disease[14-16]. Simultaneously, in combination with biologically derived materials, microfluidic devices have been used to mimic blood vessel by housing the extracellular matrix (ECM), and the ECs monolayer was formed lining the upright side of the hydrogel channel wall[17]. Therefore, the cell-cell interactions between tumor cells and ECs as well as the tumor invasion through the ECs monolayer could be investigated[10, 18-20]. To better mimic the native blood vessels, several models have been recently developed to form patent 3D endothelial monolayer, including (i) rapid casting of patterned 3D vascular networks with a gold rod[21], glass capillary[22] or biocompatible sacrificial template[23], (ii) creating of 3D lumens with basic fluidic principles[24], (iii) formation of size-controllable tubes by using a stress-induced rolling membrane technique[25], and (iv) engineering of a 3D vascular network with combining fibrillogenesis and liquid molding[26]. However, there still remain significant challenges

† [a] Key Laboratory of Analytical Chemistry for Biology and Medicine (Ministry of Education),
[a,b] College of Chemistry and Molecular Sciences, Wuhan University, Wuhan, China, 430072,
[c] Department of Oncology, Zhongnan Hosipital of Wuhan University, Wuhan, China, 430072.
[&] the first two authors contributed equally to this work.
*Corresponding author
E-mail address: whhuang@whu.edu.cn
Phone: 86 2768752149
Fax: 86 2768754067
Electronic Supplementary Information (ESI) available[Figure S1-S8; Movie S1-S2].

related to generation of simulated vascular model closely resemble the structure and functions of blood vessel with 3D endothelial monolayer and vascular walls[27].

Here, we report an artificial blood vessel implanted 3D microsystem for modeling transvascular migration of tumor cells. The versatile, cost-effective and porous cellulose-based artificial vascular microtubes are gained using chitosan sacrificial template. The transparent and elastic artificial blood vessels with well controlled inner diameter and wall thickness possess excellent biocompatibility, permeability, and mechanical characteristics, facilitating reproducing structures and functions similar to blood vessels and generating various hemodynamical conditions. Tumor transvascular migration model are constructed by fully implanted the artificial blood vessel into 3D collagen matrix, and the adhesion and transvascular migration of tumor cells have been well reconstituted.

Experimental Section

Reagents

The cell culture medium RPMI 1640, L-glutamine, HEPES and fetal bovine serum (FBS) were purchased from GIBCO (USA). 3',6'-Di(O-acetyl)-4',5'-bis[N,N-bis(carboxymethyl)-aminomethyl] fluorescein, Calcein-AM, and 3,8-Diamino-5-[3-(diethylmethylammonio) propyl]-6-PhenylPhen-anthridinium diiodide (PI) were obtained from Sigma (USA). Cell tracker Orange (CMRA), cell tracker green 5-chloromethylfluorescein diacetate (CMFDA), CD144 (VE-Cadherin) Mouse Anti-Human mAb (clone 16B1), PE conjugate, Alexa Fluor 488 phalloidin and 2-(4-Amidinophenyl)-6-indolecarbamidine dihydrochloride (DAPI) were purchased from Invitrogen (USA). Annexin V-FITC Apoptosis Detection Kit was purchased from Beyotime Institute of Biotechnology (China). FITC-dextran (*Mw*=20 kDa) and Rhodamine-dextran (*Mw*=70 kDa) were purchased from Sigma (USA). Cellulose (cotton linter pulps) with α-cellulose content of more than 95% was provided by Hubei Chemical Fiber Co. Ltd. (China). Chitosan with 90% deacetylation degree was purchased from Sinopharm Chemical Reagent Co. Ltd (China). PEO with molecular weight of 900 kDa was purchased from Jilin Global Fine Chemical Co. Ltd (China). Recombinant Human Vascular Endothecial Growth Factor (VEGF 165) and Recombinant Human Hepatocyte Growth Factor (HGF) were purchased from R&D (USA). Type I collagen was extracted from rat tail tendons and dissolved in 0.02 N acetic acid solution with 5 mg/mL according to the previous report[28]. All other chemicals unless specified were reagent grade and used without further purification.

Preparation of Cellulose and Cellulose/PEO Solution

The cellulose solution was prepared according to Zhang's method[29]. Briefly, LiOH, urea and distill water (8:15:77 by weight) was mixed evenly and then stored in a refrigerator. After the aqueous solution was precooled to -12.5 °C, cellulose was added immediately with vigorous stirring for 5 min at ambient temperature to obtain a transparent cellulose solution with concentration of 3% (w/w). The cellulose solution was then centrifugated at 7200 rpm for 15 min at 5 °C to exclude the slightly remaining undissolved part, impurities and bubbles.

PEO dissolved in LiOH/urea aqueous solution at ambient temperature to obtain PEO solution of 3% (w/w), and then the PEO solution was mixed with different ratios of cellulose solution to form cellulose/PEO mixtures.

Construction of Cellulose/Collagen Artificial Blood Vessel Implanted Microsystem

This model consists of a peristaltic pump to manipulate fluid and a cellulose/collagen artificial blood vessels implanted collagen chip. The process to prepare the model is shown in Fig. 1 and described as follows:

(1) Preparation of chitosan sacrificial template

Glass capillary was evenly precoated with chitosan layer by dipping into 3% (w/w) chitosan ethylic acid solution and then into 20% (w/w) NaOH solution to form a circular chitosan sacrificial template.

(2) Preparation of porous cellulose/collagen microtubes

Cellulose/PEO microtubes were made by dipping chitosan sacrificial template into cellulose/PEO solution with different blend ratio and then immersed in distilled water (Fig. 1B). Cellulose phase regenerated immediately and PEO phase was dissolved in water, generating macropores in the 3D scaffold of cellulose hydrogel. Then, the microtubes were immersed in 3% (w/w) ethylic acid solution to dissolve the chitosan, and porous cellulose microtubes were gained and immersed in distilled water for 24 h at room temperature to extract LiOH and urea from the porous cellulose microtubes. Finally, the microtubes were sterilized and immersed in sterile collagen solutions with concentrations of 2.5 mg/mL at 4 °C for 24 h or longer time to obtain cellulose/collagen microtubes for promoting ECs adhesion and confluent EC monolayer formation (Fig. 1C).

(3) Construction of tumor transvascular migration model

The whole microsystem for modeling transvascular migration of tumor cells including of a PDMS frame, cellulose/collagen microtubes and collagen matrix was constructed as follows: (I) A PDMS frame was firstly fabricated with controlled diameter and distance between adjacent holes. (II) Cellulose/collagen microtubes were connected with two needles which were immobilized by the holes in the PDMS frame. The other ends of the needles were connected with polyethylene tubes for interfacing (Figure 1D). To form a good connection between cellulose/collagen microtubes and needle inserted inside, the acrylic adhesive was dropped onto the connection carefully and then kept for 2 min, and tight and waterproof sealing was therefore formed when the acrylic adhesive was cured. (III) Collagen matrix was prepared on ice by mixing 2.0 mL type I rat tail liquid collagen (~5 mg/mL in 0.02 M acetic acid), 20.0 μL 2.0 M NaOH solution, and 3.0 mL 2× RPIM 1640 medium for a final collagen concentration of approximately 2.0 mg/mL. This collagen suspension was then added into the PDMS frame in which the cellulose/collagen artificial blood vessels had been immobilized, and maintained at 37 °C for 30 min in the incubator. After gelation of collagen, the microtubes were completely implanted into the collagen matrix. (IV) The HUVECs were seeded and cultured on the inner surface of cellulose/collagen microtubes to form vascular-like structure (Fig. 1E). After culturing for 2–3 days under flow conditions, the HUVECs proliferated and covered all the lining of cellulose/collagen microtubes. (V) The HCCLM9 cell lines (the patent cell lines from Li's group, (Zhongnan Hosipital of Wuhan University, China) with high metastatic capability) were seeded into the collagen matrix between artificial blood vessels for simulation of tumor intravasation; for simulation of tumor adhesion and extravasation, the HCCLM9 was perfused into the artificial vessels (Fig. 1F). All the polyethylene tubes, needles, and molds were soaked in 75 % (v/v) ethanol for 2 h and then exposed to ultra-violet (UV) light overnight in a clean hood before use.

Lab on a chip RSCPublishing

ARTICLE

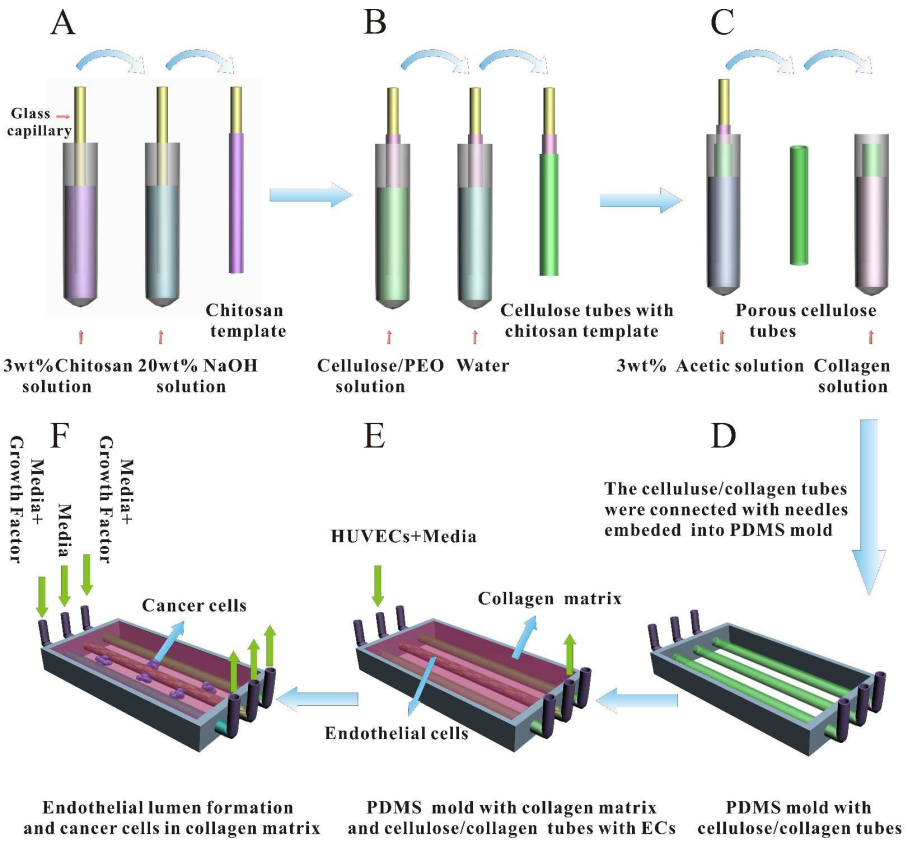

Fig. 1. Schematic diagram showing the processes of fabrication of cellulose/collagen artificial blood vessels implanted tumor transvascular migration model. Preparation of chitosan sacrificial template (A), porous cellulose microtubes (B) and porous cellulose/collagen microtubes (C). (D) Construction of vascular simulation model by implanting cellulose/collagen microtubes into collagen matrix. (E) ECs lumen formation. (F) Tumor cells seeded into the collagen matrix.

Characterization of Cellulose and Cellulose/Collagen Microtubes

(1) Scanning electron microscopy

The microtubes were frozen in liquid nitrogen and snapped immediately, and then lyophilized. The fracture surface of the microtubes was sputtered with gold, and observation of the morphology was carried out on a field emission-scanning electron microscope (FE-SEM, Sirion Tmp, Fei Co. USA).

(2) Mechanical properties

The burst strength of cellulose microtubes were measured by filling the tubes with water, keeping one end of the flow loop closed. Internal pressure of the microtubes was increased with continuous perfusion of water into the microtubes, and the pressure at point of failure was recorded as the burst pressure with a digital manometer (Nanjing Helm Sci-tech Co. Ltd, China).

(3) Gradient profile calibration

To assess the diffusivity of chemical solutions in the collagen matrix, FITC-dextran (*Mw*=20 kDa, similar to vascular endothelial growth factor, VEGF) and Rhodamine- dextran (*Mw*=70 kDa, similar to Human Hepatocyte Growth Factor HGF) were used as the indicator of the chemical gradient between the cellulose/collagen microtubes. The solutions were pumped through the microtubes to stabilize the concentrations. All the diffusion processes were observed under a fluorescent microscope (AxioObserver Z1 fluorescent microscope with camera and incubation system, ZEISS, Germany).

Human Endothelial Cells and HCCLM9 Cells Culture

The human umbilical vein endothelial cells (HUVECs) (CHI Scientific, Inc., USA) were routinely cultured using complete endothelial cell growth medium (CHI Scientific, Inc., USA). The cells were cultured for 4 days and then suspended in fresh medium with a density of 2.5×10^6 cells/mL. The elastic tubing and stainless steel needles were sterilized prior to use and interfaced the microtubes via a peristaltic pump for fluid transport. When the microtubes implanted model was prepared, it was then fixed in plastic petri dish and the evenly dispersed cell suspension (2.5×10^6 cells/mL) was quickly seeded into the microtubes within 5 min to prevent the cell sedimentation. After seeding the HUVECs at the bottom of cellulose/collagen microtubes to let them adhere for 2 h, the model was turned

upside down for a second seeding and then turned back again after 2 h to accelerate HUVECs cell monolayer formation. To facilitate the formation of confluent EC monolayer, the HUVECs were cultured at a constant flow rate close to the in vivo situations for 2-3 days in a CO_2 incubator (Heracell 150i, Thermo Scientific, USA). The pulsatile fluids were generated by a peristaltic pump (Lange, China). The HCCLM9 cells were routinely cultured using RPMI 1640 culture medium with 12 % FBS, 0.292 mg/mL L-Glutamine, 4.766 mg/mL HEPES and 0.85 mg/mL $NaHCO_3$ in the culture flask.

Endothelial Cells Migration through the Vascular Walls

HUVECs stained with cell tracker green were perfused into the middle microtube of the 3D model. When the 3D endothelial monolayer formed, the media with VEGF was perfused into the right vessels while the media without VEGF perfused into the middle and left vessels at a flow rate of 100 μL/h.

ECs migration (%)=N_{out}/N_{total} *100%, where N_{out} represents the number of ECs that migrated into collagen and the wall of cellulose/collagen artificial blood vessel, and N_{total} represents the total number of ECs.

Reconstitution of Transvascular migration of tumor cells

(1) Tumor intravasation
The model for the reconstitution of tumor intravasation consists of two independent cellulose/collagen artificial blood vessels covered by HUVECs lumen and surrounding collagen matrix. When the 3D endothelial monolayer formed, HCCLM9 cell clusters with a density of 1×10^5 cells/mL were seeded into the collagen matrix between the two vessels. The media with HGF was perfused with the concentration of 50 ng/mL under the flow rate of 100 μL/h into one simulated vascular lumen (the other cellulose/collagen microtube was perfused with media without HGF as control). The percentage of HCCLM9 cells intravasation was calculated as follows:
HCCLM9 cells intravasation (%)=N_{in}/N_{total}*100%, where N_{in} represents the number of HCCLM9 cells into the cellulose/collagen artificial blood vessels, and N_{total} represents the total number of HCCLM9 cells.
(2) Tumor adhesion and extravasation
The model for the reconstitution of tumor adhesion and extravasation is similar to the microsystem for tumor intravasation. When the 3D endothelial monolayer formed, HCCLM9 cells with a density of 5×10^5 cells/mL were perfused into the cellulose/collagen artificial blood vessel under a static flow rate of 100 μL/h and a pulse flow rate of 1.3 mL/min respectively (the other cellulose/collagen vessel without HUVECs was perfused with HCCLM9 cells as control), and the tumor adhesion was observed. When the tumor cells adhered on the surface of ECs, the tumor extravasation induced by HGF through the artificial blood vessel wall into the collagen matrix was observed. The percentage of HCCLM9 cells adhesion was calculated as follows:
Cells adhesion (%) = N_{ad}/N_{total} *100%; where N_{ad} represents the number of HCCLM9 cells adhesion on the apical of HUVECs, and N_{total} represents the total number of HCCLM9 cells.

Live Cell Imaging, Fluorescent Staining and Scanning Electron Microscopic Imaging

The viability of cultured cells was checked by Calcein-AM and PI. In the experiment for the HUVECs migration, tumor cells adhesion and transvascular migration, HUVECs and HCCLM9 cells were stained with 10 μM cell tracker green CMFDA and cell tracker orange CMRA respectively. For immunofluorescent staining of F-actin and VE-Cadherin in HUVECs, cells were stained with Alexa Fluor 488-conjugated phalloidin and CD144 (VE-Cadherin) Mouse Anti-Human mAb (clone 16B1), PE conjugate. The nuclei were stained with DAPI. The fluorescent images are obtained by an automated live cell imaging system (AxioObserver Z1 fluorescent microscope with camera and incubation system, ZEISS, Germany) and a Revolution XD confocal microscope (Andor) at 25 °C.

The cells on the inner surface of microtubes were washed with pH 7.2 PBS solution more than three times, and then fixed in 2.5% of glutaraldehyde/PBS solution for 6 h at 4 °C. After being fixed with 1% osmic acid solution, they were washed with PBS solution. The samples were dehydrated with a series of graded ethanol solution and dried in a critical point drier, and then were sputtered with gold. Observation of the morphology was carried out on a field emission-scanning electron microscope (FE-SEM, ZEISS, Germany).

Data Analysis and Quantification

All cell migration metrics were calculated by averaging the mean values of at least three models, with each model representing one independent experiment. Student's tests (two-sample, $P < 0.05$) were performed in SPSS.

Results and discussion

Fabrication and Characterization of Cellulose/Collagen Microtubes

Despite great advances achieved in investigating tumor invasion process, the mechanism is still far from being completely understood. Therefore, it is critical to develop versatile models for *in vitro* reconstitution of blood vessel incorporated tumor microenvironments. We have described a model for the simulation of blood vessel *in vitro* by forming lumens inside gelatin in our previous work[22], however, the tumor invasion could not be investigated using this model because the ingrowth of ECs and tumor cells is restricted in stiff gelatin gels[30]. Here, we propose the development of transparent and elastic cellulose porous cellulose/collagen microtubes as artificial vascular microtubes by gelation of cellulose solution on a round chitosan sacrificial rod template, and there with present a model that consists of the artificial blood vessel and surrounding collagen as the matrix for tumor growth. As the most abundant natural polymers, cellulose has excellent biocompatibility and biodegradability, and cellulose hydrogel prepared by alkli/urea systems possesses good mechanical strength and toughness with porous structure[31-33]. However, cellulose hydrogel provide the pore size from only 200 to 500 nm after gelation in water[34], which is not enough for cells migration through the microtubes. Thus, PEO as a porogen was added to the cellulose solution to enlarge the pore size. Interconnected pores ranging from 10 to 75 μm were prevalent with increasing percentage of PEO from 10% to 60%

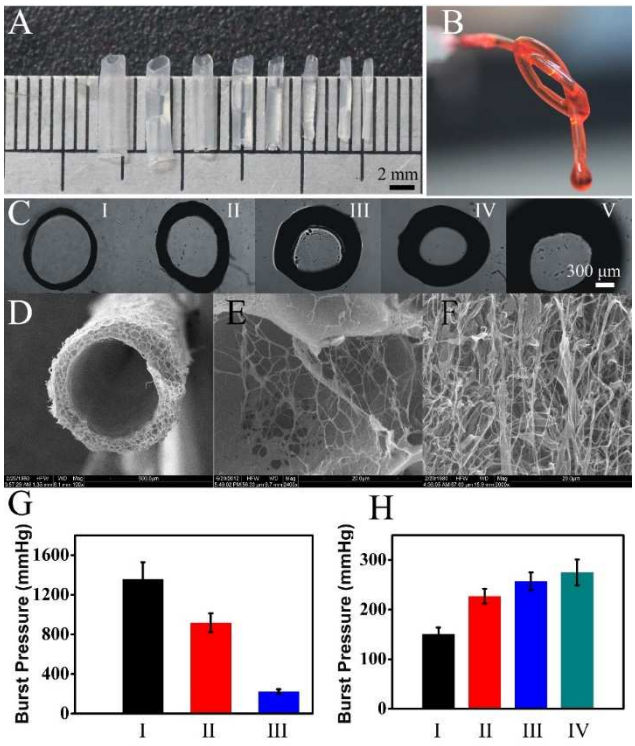

Fig. 2. Characterization of cellulose-based artificial blood vessels. Photograph of cellulose microtubes (A) at a range of approximate inner diameters (from left to right): 2.1, 1.8, 1.6, 1.4, 1.1 mm, 900, 600 and 500 μm; (B) filling with red dye. (C) Microscopic images of cellulose microtubes with different wall thickness. From I to V: 100, 200, 350, 400 and 550 μm. (D-F) SEM images of the section (D, E) and inner (F) of the cellulose/collagen microtubes obtained from chitosan sacrificial template. (G) Burst pressure of (I) cellulose microtubes, (II) cellulose microtubes using chitosan sacrificial template, and (III) cellulose/PEO (6:4) microtubes using chitosan sacrificial template, wall thickness was 200 μm (n=5). (H) Burst pressure of cellulose/PEO (6:4) microtubes using chitosan sacrificial template filled with different concentrations (from I to IV, 0, 1.0, 2.5 and 5 mg/mL) of collagen, wall thickness was 150 μm (n=5).

(w/w), efficiently improving the permeability of 3D scaffold for cells migration (Fig. S1).

Glass capillary could be used as template for rapid casting lumen structures[30,35]. However, the difference in diffusion rate of water (as coagulant) inside 3D hydrogel structure during gelation process[34]and the interface effect using smooth capillary[36] could only generate very small pores (300~1000 nm) lining the cellulose microtube (Fig. S2A, D). Therefore, we developed a strategy by precoating chitosan on glass capillary to form a sacrificial template (Fig. S2B, C). The chitosan hydrogel template with a rough surface can support enough water for coagulation of cellulose near the template, generating rough and highly-porous lining of cellulose microtubes with pore size from 10 μm to 35 μm (Fig. S2E).

Transparent and elastic microtubes with different dimensions were obtained by this method. The inner diameters of cellulose/collagen tubes could be controlled by the diameters of the templates, and the thickness could be well controlled by both the concentration of cellulose solution and the cellulose/PEO ratio (Fig. 2A-C, Fig. S3). To better simulate the structures and functions of blood vessel *in vivo*, collagen was filled into the 3D scaffold of cellulose tubes for mimicking the vascular cell biology community and providing cell-responsive characteristics. As shown in SEM images, both the section (Fig. 2D, E and Fig. S2C, G-I) and inner (Fig. 2F) of cellulose/collagen microtubes are filled with collagen microfibers. Various vessels such as artery, vein and capillaries, have their unique structure and functions with different diameter and thickness. This model allows us to flexibly regulate the formation and dimensions of cellulose/collagen tubes by varying a number of parameters, therefore facilitating on-demand construction of vascular graft with different functions.

Burst pressures of various cellulose or cellulose/collagen microtubes were measured to test the mechanical characteristics of microtubes. The cellulose microtubes using glass capillary as template had the highest burst pressures of 1358±171 mmHg, significantly approaching to those of human saphenous veins (1680±307 mmHg)[37]. Burst strengths of cellulose and cellulose/PEO (6:4) microtubes (wall thickness, 200 μm) with chitosan template were decreased to 918±95 and 240±20 mmHg respectively (Fig. 2G). The filling of collagen into the 3D scaffold of cellulose microtube could efficiently improve the mechanical strength. Burst pressures of cellulose/PEO (6:4) microtubes (wall thickness, 150 μm) with chitosan template after being treated by collagen with different concentration of 0, 1, 2.5 and 5 mg/mL were 151±13, 227±15, 257±18 and 275±26 mmHg, respectively (Fig. 2H). These values were enough to mimic blood vessels *in vivo* with physiological pressures of approximately 100–140 mmHg (coronary artery during systole) or 15–40 mmHg (capillary blood pressure)[38]. The cellulose/collagen microtubes provide proper mechanical characteristics for simulation of blood vessels, and the excellent balance between porosity (the average pore sizes inside cellulose/PEO (6:4, w/w) microtubes were 48±8μm) and mechanical properties allows the investigation of soluble factor diffusion and cell migration across the artificial blood vessel wall under the normal hemodynamic conditions. It indicates that these microtubes may meet the needs of porous scaffolds for vascular tissue engineering applications[39] and investigation of tumor transvascular migration *in vitro*.

3D Vascular Lumen Formation and Hemodynamic Simulation

The transparent, elastic and porous cellulose/collagen microtubes indicated that they were qualified to mimic blood vessels *in vitro*. Therefore, cellulose/collagen artificial blood vessels were fully encapsulated within the collagen matrix to construct tumor microenvironment consisting of blood vessels (distance between adjacent vessels could well be controlled) and surrounding matrix (Fig. 3A). To test the permeability of vascular wall and simulate the diffusion of soluble factors in the extravascular matrix, the gradient generation of FITC-labeled dextran (*Mw* =20 kDa) and Rhodamine- dextran(*Mw* =70 kDa) were used as the indicator of the chemical gradient between the microtubes (Fig. 3B, C, Fig. S4). The results showed that the gradient of FITC-dextran and Rhodamine-dextran stabilized to form equilibrium profiles after 8 h and could keep stable in 48 h.

In order to obtain 3D vessel lumens with endothelial monolayer, HUVECs were seeded and cultured on the inner surface of the microtubes for 2-3 days under flow conditions. The confocal microscopic images of HUVECs stained by Calcein-AM demonstrate confluent HUVECs monolayer is formed lining the artificial blood vessels (Fig. 3D), indicating the simulated vessel lumens with 3D endothelial monolayer

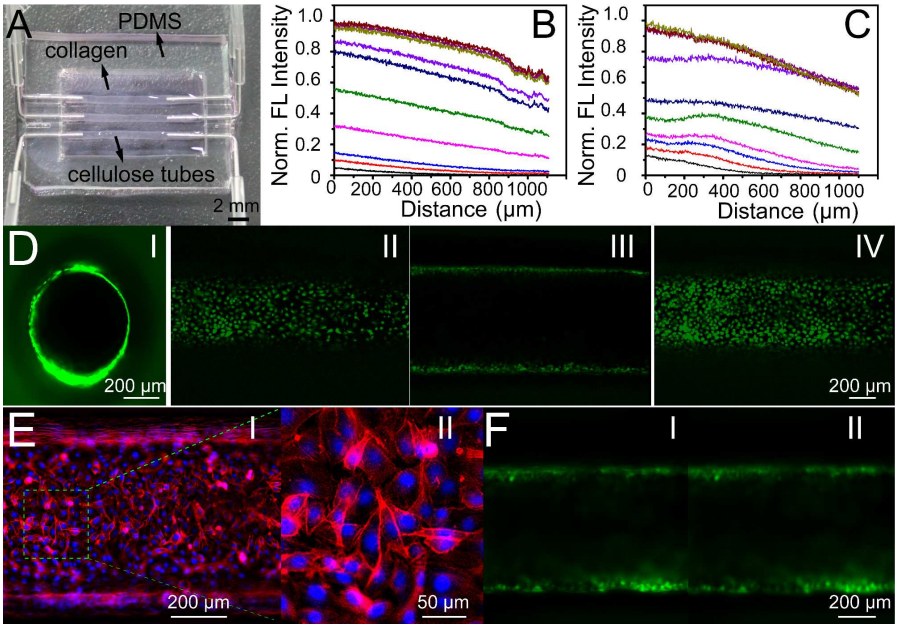

Fig. 3. Blood vessels simulation. (A) Photograph showing the implant of three cellulose/collagen artificial blood vessels into collagen matrix. (B,C) Development of concentration gradient profiles showing the gradient generation of FITC-dextran (*Mw* = 20 kDa) (B) and Rhodamine-dextran(*Mw*=70 kDa)(C) between adjacent cellulose lumens over time. The time from bottom to top: 0, 15, 30, 45min, 1, 2, 6, 8, 24, 48h. (D) Fluorescent microscopic images of HUVECs cultured for 48 h. Green: Calcein-AM staining to show cell viability. Volume-rendered cross section of ECs (I), the ECs at the top (II), middle (III) and bottom (IV) of the lumen. (E) VE-Cadherin (red) and DAPI (blue) staining to show the confluency of the endothelial monolayer; (F) Fluorescent microscopic images of ECs on the lining of cellulose artificial blood vessels under pulsatile flow conditions, (I): Systolic (II): Diastolic (frequency 1 Hz, flow rate 1.3 mL/min).

could be easily generated owning to improved cytocompatibility by filling collagen into the 3D scaffold (Movie S1, stained by Alexa Fluor 488 phalloidin). Furthermore, viability experimental results (>99% cell viability) showed excellent cytocompatibility of cellulose/collagen microtubes (Fig. S5). The endothelial cells were cultured under flow conditions and the SEM images were obtained (Fig. S6). It can be seen that the endothelial lining in the cellulose/collagen microtube lumen formed a confluent monolayer. The vascular endothelial-cadherin (VE-Cadherin) antibody was used to characterize the VE-cadherin expression in the connections between these ECs, and the immunefluorescent results (Fig. 3E) demonstrated the presence of VE-Cadherin and the formation of integrated endothelial layer on the surface of a round cellulose/collagen tube.

The hemodynamic characteristics of artificial blood vessel implanted in the collagen matrix such as adaptive response of endothelial cells to shear stress under pulse conditions were investigated. The elastic artificial blood vessel produced a peak pressure of 100 mmHg and an end diastolic pressure of 10 mmHg at a rate of 60 bpm (Fig. 3F and Movie S2). The cell adhesion capability was tested, and only 5% of the cells were detached from the lining of cellulose under this pulse conditions after 1 h. The results demonstrate the validity of HUVECs culture and vascular simulation model under strong shear stress tolerance and adaptation, which is important to maintain the structures and functions of the HUVECs.

VEGF Stimulate the Endothelial Cells Migration across the Artificial Blood Vessel Wall

To assess cellular migration through the artificial blood vessel wall in response to concentration gradients of VEGF, HUVECs were perfused into the middle microtube to form 3D endothelial

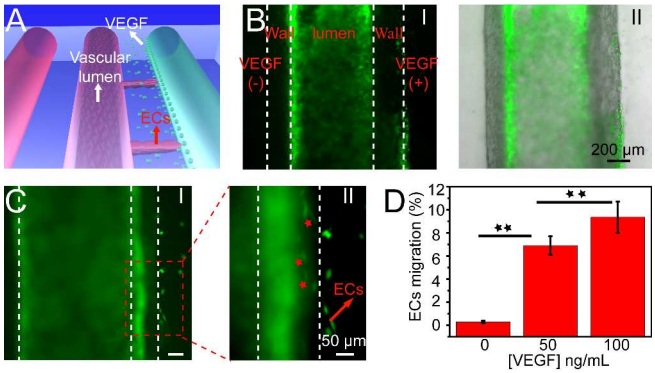

Fig. 4. Endothelial cells migration across the artificial blood vessel wall into the surrounding collagen matrix. (A) Schematic of endothelial cells migration in response to VEGF. (B) Microscopic images of HUVECs response in the presence and absence of VEGF (I) Fluorescence field (II) Bright field + fluorescence field. (C) Fluorescent image showing HUVECs migration from the simulated vascular lumen to the collagen induced by VEGF (scale bar: 100 μm (I)). (D) Percentage of HUVECs migration into surrounding collagen matrix under different concentration of VEGF. (** P<0.05)Error bar: SEM, sample number n=3.

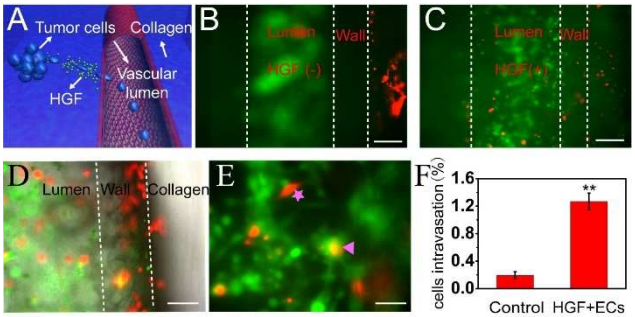

Fig. 5. Intravasation of HCCLM9 cells from the surrounding collagen into simulated vascular lumen. (A) Schematic of HCCLM9 cells intravasation in response to HGF. Fluorescent images showing the intravasation of HCCLM9 cells in the absence (B) and presence of HGF (C), HUVECs: green, HCCLM9: red, (scale bar: 200 μm). (D) Fluorescent image of the HCCLM9 cells in response to HGF across the artificial blood vessel wall. (E) Fluorescent image of HCCLM9 cells and HUVECs, (scale bar: 100 μm). ▲: Tumor cells on the basal side of the endothelium ★: Tumor cells on the apical of the endothelium (F) Percentage of HCCLM9 cells intravasation from the surrounding collagen into simulated vascular lumen in the presence (n=6) and absence of HGF (n=3) (** $P<0.05$) Error bar: SEM.

monolayer, and the perfusion of media with VEGF in the right microtube formed stable and predictable gradients between the middle and right microtubes (Fig. 4A, the left microtube without VEGF perfusion as control). The porous structure for cell migration has been firstly demonstrated by observation of ECs migrating across the artificial blood vessel wall toward VEGF gradient. Obviously, upon VEGF stimulation, HUVECs migrated from the lining of the cellulose/collagen artificial blood vessel to the 3D matrix and found in the scaffold of the wall and surrounding collagen matrix after 24 h when the wall thickness was 150 μm (Fig. 4B, C). During the migration process, HUVECs bodies were elongated toward spindle-shaped morphologies inside the cellulose scaffold and collagen by the induction of VEGF. It was found that 0.29 ± 0.11% HUVECs migrated outside the lumen without induction of VEGF, while when the concentration of VEGF in the right microtube were 50 ng/mL and 100 ng/ml, 6.9 ± 0.80% and 9.35 ± 1.35% HUVECs migrated up VEGF concentration gradients into the surrounding collagen matrix (Fig. 4D). The result demonstrates the excellent cellular permeability of porous artificial blood vessel and VEGF efficiently promotes the migration of HUVECs toward the concentration gradients.

Tumor Cells Intravasation across the Artificial Blood Vessel Wall into the Lumen

As a critical step of tumor metastasis, intravasation refers to the invasion of tumor cells through the basal membrane into a blood or lymphatic vessel. The model for the reconstitution of tumor intravasation consists of two independent cellulose/collagen artificial blood vessels covered by HUVECs lumen which was used to mimic structure and barrier functions of native blood vessel wall (Fig. 5A). When the 3D endothelial monolayer formed, HCCLM9 cell clusters were seeded into the collagen matrix between the two artificial blood vessels. The media with HGF, which has been shown to participate in tumorigenesis and metastasis in vivo [40,41] was perfused into one simulated vascular lumen to induce the invasion of HCCLM9 cells (Fig. 5B, the microtube without HGF perfusion as control).

Obviously, upon the stimulation of HGF, HCCLM9 cells migrated from the 3D matrix into the lumen (Fig. 5C) and found both in the artificial blood vessel wall scaffold and on the basal side or apical of HUVECs after 48 h (Fig. 5D, E), indicating that the HGF promotes the invasion and metastasis of hepatoma cells[42]. The tumor cells morphology changed from ellipsoid to spindle-shaped through the surrounding collagen matrix and 3D scaffold in the artificial blood vessel wall, and then majority of HCCLM9 cells recovered after completely invaded into the lumen. Intravasation was an inefficient event and occurred for a small fraction of the tumor cells[20]. The experimental results indicate that a significantly higher percentage of tumor cells invaded (1.27±0.12%) in the presence of HGF compared to control condition (0.20±0.05%) (Fig. 5F). The migration rate (6 μm/h) of tumor cells in the 3D scaffold of the artificial blood vessel wall is much slower than it in pure collagen matrix (13 μm/h), indicating that tumor cells could successfully break through the barrier of the artificial blood vessels but with a slower invasion rate.

Tumor intravasation is the critical step of tumor metastasis leading to tumor cells spread from primary sites to other sites through the blood stream. In vivo imaging has showed that tumor cells invade into blood vessel[43], and tumor intravasation occurs on the capillaries[44] or the microvessels[45]. Currently available in vitro models usually involve tumor cell invading the planner or vertical HUVECs monolayer on hydrogel matrix, and fail to reconstitute tumor cells transverse 3D ECs monolayer lining the vascular wall and underlying basement membrane. Here, our in vitro models using natural polysaccharide scaffold with collagen stuffing well mimic the structure and function of vascular wall of microvessels with 3D endothelial monolayers.

Tumor Cells Adhesion and Extravasation across the Artificial Blood Vessel Wall

Tumor adhesion on the apical of endothelium and extravasation of tumor cells through the endothelium barrier and vessel walls are essential steps in the metastatic process and determine the metastatic spread[20,40]. Fig. 6A shows the model for the reconstitution of tumor adhesion and extravasation. When the 3D endothelial monolayer formed, HCCLM9 cells were perfused in the artificial blood vessel under flow rate of 100 μL/h (shear stress of 0.03 dye/cm^2), and 10.40%±0.79% cells were adhesive to apical endothelial of artificial blood vessels after 1h while only 1.33±0.11% tumor cells could be adhered on the native surface of cellulose/collagen microtubes. Under a pulse flow rate (1.3 mL/min, shear stress of 13 dye/cm^2) with a pulse rate of 60 bpm, no tumor cells was found on the native surface of cellulose/collagen microtubes while 3.14±0.32% HCCLM9 cells adhered to apical endothelial of artificial blood vessels (Fig. 6B, I). Previous studies indicated that tumor adhesion to ECs occurs in the blood stream and is greatly affected by various parameters such as shear stress and chemical signals. Our results demonstrated that, compared to native cellulose microtubes, the simulated vascular lumen with 3D endothelium showed dramatically increased tumor adhesion under both static and pulse flow conditions, indicating specific interaction between HUVECs and tumor cells facilitate tumor adhesion in the vasculature of specific organs and promote the

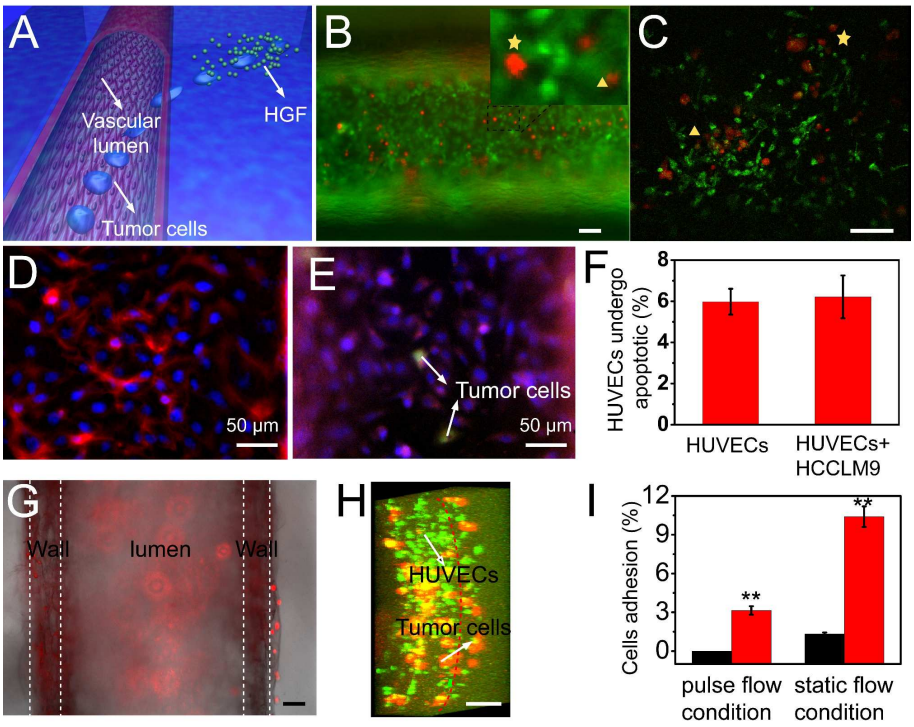

Fig. 6. Tumor cells adhesion on the HUVECs and extravasation across the artificial blood vessel wall into the collagen. (A) Schematic of HCCLM9 cells adhesion and extravasation in response to HGF. (B) Tumor cells adhesion on the apical of cellulose lumen with HUVECs. (C) Tumor cells on the basal side of the endothelium. ★: Tumor cells on the basal side of the endothelium ▲: Tumor cells on the apical of the endothelium. (D,E) VE-Cadherin (red) and DAPI (blue) staining in absence (D) and presence (E) of HCCLM9 cells, HCCLM9 cells were stained with cell tracker green. (F) Apoptosis rate of HUVECs in the presence and absence of HCCLM9 cells ($P>0.05$). (G,H) Fluorescent image (G) and confocal image (H) of tumor cells extravasation across the artificial blood vessel wall into the collagen (scale bar: 50 μm). (I) Percentage of tumor cells adhesion in the lining of cellulose in the presence (red) and absence (black) of HUVECs under static flow conditions and pulse flow conditions. ($P<0.05$) Error bar: SEM, sample number n=3, Scale bar: 100 μm.

adhesion of tumor cells to endothelial monolayer. The VE-cadherin expression in the connections between these HUVECs and apoptosis rates of HUVECs in the presence and absence of HCCLM9 were investigated by fluorescent (Fig. 6D-F) and SEM imaging (Fig. S7). The results showed significantly less VE-cadherin expression after adherence of HCCLM9 cell on HUVECs for 24 h, and the SEM result indicated the disruption of the confluent HUVECs monolayer. Furthermore, apoptosis rates of HUVECs (Fig. S8) in the presence and absence of HCCLM9 were not obviously different. The combined results demonstrated that the HCCLM9 extravasation was realized by breaking the integrity of confluent HUVECs monolayer rather than causing HUVECs apoptosis.

HCCLM9 cells exhibit obvious cell shape changes when they adhered on the apical of endothelium. Consequently, the confluency of endothelial monolayer was broken, which led to the invasion of the tumor cells into the 3D matrix through the endothelium barrier up the concentration gradients of HGF (Fig. 6G,H) after 48 h. Therefore, *in vitro* tissue-engineered blood vessel model is capable of reproducing the process of tumor cell adhesion and extravasation under the physiological hemodynamic conditions.

Taken together, the results demonstrated that this *in vitro* models using natural polysaccharide scaffold with collagen stuffing could well mimic the structure and function of vascular wall of microvessels with 3D endothelial monolayers. Furthermore, hemodynamic parameters such as flow rate, shear stress and pulse frequency similar to native blood vessels were easily generated. The results show that HCCLM9 cells could successfully transverse the 3D HUVECs monolayer lining the artificial blood vessel wall under induction of HGF with slow migration rate, indicating that the barrier function of vascular wall efficiently delay the tumor migration. HGF, as a multi-functional cytokine on cells of mainly epithelial origin, has been shown to have a major role in tumorgenesis and tissue regeneration[41], however, there are still many arguments existing in the effects of HGF with different concentration on the liver cancer metastasis. Our experiment result indicated that the HGF with the concentration less than 50 ng/mL efficiently promotes the invasion of hepatoma cells[42].

Conclusions

In this work, we develop an artificial blood vessel implanted 3D microsystem for modeling transvascular migration of tumor cells. The transparent, elastic and porous cellulose-based microtubes with 3D endothelium well mimic the structure and functions of blood vessel wall, and the artificial blood vessel also could easily replicate the vascular hemodynamics. The artificial blood vessels were fully implanted into 3D collagen matrix to construct tumor microenvironment for modeling the tumor adhesion and transvascular migration. The results

demonstrate that HGF promotes the migration of hepatoma cells and specific interaction between ECs and tumor cells promotes the adhesion of tumor cells to endothelial monolayer, leading to disruption of confluent ECs monolayer for transvascular migration of tumor cells. The success in reconstruction of vascular structure as well as modeling of tumor cell transvsacular migration would open up opportunities for study of tumor-vascular interaction.

Acknowledgements

This work was supported by the National Basic Research Program of China (973 Program, No. 2012CB720603), National Science Foundation of China (Nos. 21375099, 31070995), Specialized Research Fund for the Doctoral Program of Higher Education (20120141110031) and the Fundamental Research Funds for the Central Universities (2042014kf0192).

References

1 E. Quintana, E. Piskounova, M. Shackleton, D. Weinberg, U. Eskiocak, D. R. Fullen, T. M. Johnson and S. J. Morrison, *Sci. Transl. Med.* 2012, 4, 159ra149.
2 S. Sutcliffe and G. A. Colditz, *Nat. Rev. Cancer* 2013, 13, 208-218.
3 P. Saharinen, L. Eklund, K. Pulkki, P. Bono and K. Alitalo, *Trends. Mol. Med.* 2011, 17, 347-362.
4 A. Zaravinos, J. Radojicic, G. I. Lambrou, D. Volanis, D. Delakas, E. N. Stathopoulos and D. A. Spandidos, *J. Urol.* 2012, 188, 615-623.
5 P. Carmeliet and R. K. Jain, *Nature* 2000, 407, 249-257.
6 I. J. Fidler, *Nat. Rev. Cancer* 2003, 3, 453-458.
7 C. A. Staton, S. M. Stribbling, S. Tazzyman, R. Hughes, N. J. Brown and C. E. Lewis, *Int. J. Exp. Path.* 2004, 85, 233-248.
8 J. Condeelis and J. E. Segall, *Nat. Rev. Cancer* 2003, 3, 921-930.
9 Y. Zheng, J. Chen, M. Craven, N. W. Choi, S. Totorica, A. Diaz-Santana, P. Kermani, B. Hempstead, C. Fischbach-Teschl, J. A. Lopez and A. D. Stroock, *Proc. Natl. Acad. Sci. USA* 2012, 109, 9342-9347.
10 I. K. Zervantonakis, S. K. Hughes-Alford, J. L. Charest, J. S. Condeelis, F. B. Gertler and R. D. Kamm, *Proc. Natl. Acad. Sci. USA* 2012, 109, 13515-13520.
11 X. Peng, F. A. Recchia, B. J. Byrne, I. S. Wittstein, R. C. Ziegelstein and D. A. Kass, *Am. J.* Physiol. *Cell Physiol.* 2000, 279, C797-C805.
12 F. Bruyère, F. Bruyere, L. Melen-Lamalle, S. Blacher, G. Roland, M.Thiry, L. Moons, F. Frankenne, P. Carmeliet, K. Alitalo, C. Libert, J. P. Sleeman and J. M. Foidart, Noel, A. *Nat. Methods* 2008, 5, 431-437.
13 L. L. Y. Chiu, M. Montgomery, Y. Liang, H. J. Liu and M. Radisic, *Proc. Natl. Acad. Sci. USA* 2012, 109, E3414-E3423.
14 G. A. Giridharan, M. D. Nguyen, R. Estrada, V. Parichehreh, T. Hamid, M. A. Ismahil, S. D. Prabhu and P. Sethu, *Anal. Chem.* 2010, 82, 7581-7587.
15 R. Estrada, G. A. Giridharan, M. D. Nguyen, T. J. Roussel, M. Shakeri, V. Parichehreh, S. D. Prabhu and P. Sethu, *Anal. Chem.* 2011, 83, 3170-3177.
16 E. W. K. Young and C. A. Simmons, *Lab Chip* 2010, *10*, 143-160.
17 G. S. Jeong, S. Han, Y. Shin, G. H. Kwon, R. D. Kamm, S. H. Lee and S. Chung, *Anal. Chem*. 2011, 83, 8454–8459.
18 C. Zheng, L. Zhao, G. Chen, Y. Zhou, Y. Pang and Y. Huang, *Anal. Chem.* 2012, 84, 2088-2093.
19 Q. Zhang, T. J. Liu and J. H. Qin, *Lab Chip* 2012, 12, 2837-2842.
20 M. K. Shin, S. K. Kim and H. Jung, *Lab Chip* 2011, 11, 3880-3887.
21 N. Sadr, M. J. Zhu, T. Osaki, T. Kakegawa, Y. Z. Yang, M. Moretti, J. Fukuda and A. Khademhosseini, *Biomaterials* 2011, 32, 7479-7490.
22 L. M. Li, X. Y. Wang, L. S. Hu, R. S. Chen, Y. Huang, S. J. Chen, W. H. Huang, K. F. Huo and P. K. Chu, *Lab Chip* 2012, 12, 4249-4256.
23 J. S. Miller, J. S. Miller, K. R. Stevens, M. T. Yang, B. M. Baker, D. H. T. Nguyen, D. M. Cohen, E. Toro, A. A. Chen, P. A. Galie, X. Yu, R. Chaturvedi, S. N. Bhatia and C. S. Chen, *Nat. Mater.* 2012, 11, 768-774.
24 L. L. Bischel, E. W. K. Young, B. R. Mader and D. J. Beebe, *Biomaterials* 2013, 34, 1471-1477.
25 B. Yuan, Y. Jin, Y. Sun, D. Wang, J. S. Sun, Z. Wang, W. Zhang and X. Y. Jiang, *Adv. Mater.* 2012, 24, 890-896.
26 X. Mu, W. F. Zheng, L. Xiao, W. Zhang and X. Y. Jiang, *Lab Chip* 2013, 13, 1612-1618.
27 J. G. Nemeno-Guanzon, S. Lee, J. R. Berg, Y. H. Jo, J. E. Yeo, B. M. Nam, Y. G. Koh and J. I. Lee, *J. Biomed. Biotechnol.* 2012, 956345.
28 N. Rajan, J. Habermehl, M. F. Cote, C. J. Doillon and D. Mantovani, *Nat. Protoc.* 2006, 1, 2753-2758.
29 J. Cai and L. N. Zhang, *Macromol Bio Sci* 2005, 5, 539-548.
30 Y. C.Chen, R. Z. Lin, H. Qi, Y. Z. Yang, H. J. Bae, J. M. Melero-Martin and A. Khademhosseini, *Adv. Funct. Mater.* 2012, 22, 2027-2039.
31 C. Y. Chang, B. Duan and L. N. Zhang, *Polymer* 2009, (50), 5467-5473.
32 C. Y. Chang, M. He, J. P. Zhou and L. N. Zhang, *Macromolecules* 2011, 44, 1642–1648.
33 Y. Pei, X. Y. Wang, W. H. Huang, P. Liu and L. N. Zhang, *Cellulose* 2013, 20, 1897-1909.
34 R. Li, L. N. Zhang and M. Xu, *Carbohyd. Polym.* 2012, 87, 95-100.
35 J. Cai and L. N. Zhang, *Macromol. Biosci.* 2005, 5, 539-548.
36 Y. Mao, J. P. Zhou, J. Cai and L. N. Zhang, *J. Membrane Sci.* 2006, 279, 246-255.
37 N. L'Heureux, N. Dusserre, G. Konig, B. Victor, P. Keire, T. N. Wight, N. A.F. Chronos, A. E. Kyles, C. R. Gregory, G. Hoyt, R. C. Robbins, and T. N. McAllister, *Nat. Med.* 2006, 12, 361-365.
38 S. A. Williams, S. Wasserman, D. W. Rawlinson, R. I. Kitney, L. H. Smaje and J. E. Tooke, *Clin. Sci. 1988, 74, 507-512.*
39 K. A. Paschos, D. Canovas and N. C.Bird, *Cell Signal* 2009, 21, 665-674.
40 R. Haddad, K. E. Lipson and C. P. Webb, *Anticancer Res.* 2001, 21, 4243-4252.
41 D. P. Bottaro, J. S. Rubin, D. L. Faletto, A. M. Chan, T. E. Kmiecik, G. F. Vande Woude and S. A. Aaronson, *Science* 1991, 251, 802–804.
42 V. Neaud, S. Faouzi, J. Guirouilh, B. Le Bail, C. Balabaud, P. Bioulac-Sage and J. Rosenbaum, *Hepatology* 1997, 26, 1458-1466.
43 J. P. Quigley and P. B. Armstrong, *Cell* 1998, 94, 281–284.
44 A. F. Chambers, I. C. MacDonald, E. E. Schmidt and V. L. Morris, *Adv. Cancer Res.* 2000, 79, 91-121.
45 S. Scherbarth and F. W. Orr, *Cancer Res.* 1997, 57, 4105-4110.

Graphical abstract

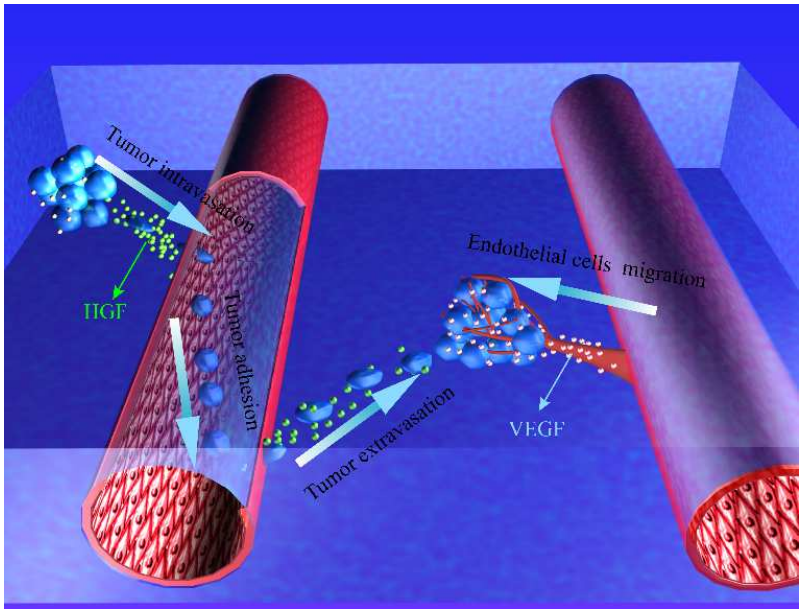

We developed an artificial blood vessel implanted 3D microfluidic system for reproducing vascular functions and transvascular migration of tumor cells. Based on this model, the adhesion and transvascular migration of tumor cells across the artificial blood vessel have been well reproduced under the normal hemodynamic conditions.

